DOI: 10.1021/ma902294k

Macromolecules
COMMUNICATION TO THE EDITOR

Programmable Nanoparticle Assembly via Polymer Single Crystals

Bing Li, Bingbing Wang, Robert C. M. Ferrier, Jr., and Christopher Y. Li*

Department of Materials Science and Engineering, Drexel University, Philadelphia, Pennsylvania 19104

Received October 14, 2009
Revised Manuscript Received November 8, 2009

Introduction. Nanoparticles (NPs) are arguably the most important building blocks for future advanced functional materials.[1−3] To transfer their fascinating optical, electronic and magnetical properties from nano- to meso- and/or macroscales, these NPs need to be assembled into desired structures for targeted applications.[2,4−8] Despite extensive study in the field, it remains a challenging task to pattern NPs into ordered structures in a controlled manner. Herein we report a novel approach for massive production of NP sheets with programmable patterns. Uniform NP sheets were fabricated by using an *in situ* polymer crystallization method. Tailor-made, free-standing frames and chains containing single or multiple types of NPs have been obtained. This unprecedented assembly approach paves the way to massive production of complex NP structures for applications ranging from nanodevices to biology.

Soft matter has been widely used to pattern NPs into complex structures.[6−8] For instance, surfactants have been used to fabricate uniform three-dimensional (3D) NP crystals,[7] two-dimensional (2D) monolayer and multiple layers[9,10] and one-dimensional (1D) NP/nanorod chains.[11−13] DNA and polypeptide have shown great potential to direct NP assembly and numerous assembled NP structures including free-standing sheets have been reported.[14−18] Block copolymers, both in solution and bulk state, have also been used to guide NP assembly.[4,5,8,19−22] Typically, NPs are sequestered in one domain and/or the boundary of the microphase separated block copolymers, replicating the nanoscale ordered structure. However, massive production of NP sheets with precise positional control at different length scales has not yet been realized. It is particularly challenging to pattern multiple types of NPs into one ordered structure.

Polymer single crystals can be readily obtained by crystallization from a dilute solution.[23] A typical polymer single crystal has lamellar shape, approximately 10 nm thick and a few nanometers to a few micrometers wide. Just 1 g of crystalline polymer may produce over 10^{13} identical micro-sized sheets freely suspended in solution. Formation of polymer single crystals induced by one-dimensional nanomaterials has been recently investigated.[22,24−29] The interplay between NPs and polymer single crystals is not obvious although metal NPs formed by vapor deposition on the surface of inorganic and polymer crystals have been used to reveal crystal defect structures since 1958.[30,31] Nevertheless, if end-functionalized polymers are used to form single crystals, the end groups are often excluded onto the crystal surface. In this context, if we consider inert polymer lamellae as "nanopaper", polymer single crystals with functional groups on the surface resemble "nanotape", which can be used to harvest different nanoscale objects including NPs, biomolecules, viruses, etc. Recently, we demonstrated that gold nanoparticles (AuNPs) can be adsorbed onto the thiol-terminated poly(ethylene oxide) (HS−PEO) single crystals by mixing gold colloids with single crystals.[32−34] This NP adsorption process occurred *after* crystallization of HS−PEO and the single crystals were fully covered by AuNPs. In this letter, we demonstrate that much more complex NP patterns on these single crystals can be obtained by in situ assembling NPs during polymer crystallization. We were able to precisely control three features of the patterns at different length scales, namely, the inter-NP distance (previously demonstrated),[32] the width and length of the frames/chains and the interframe/chain distance. The ability to pattern different NPs on one single crystal paves the way to synthesizing multifunctional polymer/NP hybrids.

Experimental Section. *Materials.* Thiol-terminated poly(ethylene oxide) methyl ether (HS−PEO), number-average molecular weight $M_n = 2000$ g/mol, was purchased from Polymer Source Inc. HS−PEO, $M_n = 5000$ g/mol, was purchased from JenKem Technology USA. Hydroxyl-terminated PEO, $M_n = 5000$ g/mol, was purchased from Sigma-Aldrich, Inc. Quantum dots (CdSe@ZnS, 5 nm, 10 mg/mL in toluene) were purchased from Evident Technologies, Inc. Pentyl acetate was purchased from Sigma-Aldrich, Inc. and was distilled before use.

Methods

Preparation of PEO Single Crystals Using the Self-Seeding Method. A 1.2 mg sample of PEO was dissolved in 3.0 g of pentyl acetate at 60 °C for 10 min. Then the solution was quenched to 5 °C overnight. The resulted suspension was brought to the self-seeding temperature (38 °C for $M_n =$ 2000 g/mol and 44 °C for $M_n = 5000$ g/mol) for 10 min to obtain the crystalline seeds. The solution was then left at room temperature and crystallized for 24 h. The final suspension was filtered to remove uncrystallized PEO.

Preparation of Gold Colloid in Pentyl Acetate. Gold colloid was synthesized by following the procedure reported by O'Brien.[35] The synthesized 5 nm AuNPs were dispersed in pentyl acetate with a concentration at 0.1 mg/mL.

Preparation of Iron(II, III) Oxide (Magnetite) Nanoparticles. Magnetite NPs were synthesized by following the procedure reported by Hyeon.[36] The synthesized 15 nm magnetite NPs were dispersed in pentyl acetate with a concentration at 1.0 mg/mL.

Preparation of Uniform AuNP Sheets by Mixing. The method was reported previously.[32] Briefly, 0.5 g of the suspension of filtered HS−PEO single crystals was mixed with 0.5 g of gold colloid in pentyl acetate for 24 h. The mixture was filtered to remove the unbound NPs.

Preparation of AuNP Frames. First, 0.5 g of gold colloid in pentyl acetate was added to 3.0 g of 0.04 wt % HS−PEO ($M_n = 2000$ g/mol) solution at various t_d (defined later). The mixture continued to crystallize for 24 h. The final suspension was filtered to remove uncrystallized PEO and unbound AuNPs.

Preparation of Single Crystals of AuNP−PEO Conjugates. A 1.0 g sample of 0.08% HS−PEO ($M_n = 2000$ g/mol) solution in pentyl acetate was mixed with 0.5 g of gold

*Corresponding author. E-mail: chrisli@drexel.edu. Telephone: 215-895-2083. Fax: 215-895-6760.

 Published on Web 11/23/2009

colloid at room temperature for 30 h. A red precipitate composed of the single crystals of AuNP−PEO conjugates was obtained.

Preparation of AuNP Frames around Preformed Single Crystals. Here, 1.0 g of 0.08 wt % HS−PEO (M_n = 2000 g/mol) solution in pentyl acetate and 0.5 g of gold colloid in pentyl acetate were added subsequently to 1.0 g of 0.02 wt % filtered HS−PEO (M_n = 5000 g/mol) single crystal suspension. The mixture was allowed to crystallize at room temperature for 28 h. The final suspension was filtered to remove uncrystallized PEO and unbound AuNPs.

Preparation of AuNP Frames Formed around Preformed Single Crystals by AuNP−PEO Conjugates. A 1.0 g sample of 0.08% HS−PEO (M_n = 2000 g/mol) solution in pentyl acetate was mixed with 0.5 g of gold colloid at room temperature for 30 h. The red precipitate was redissolved at 60 °C. The resultant solution was quickly added to 1.0 g of 0.02 wt % filtered HS−PEO (M_n = 5000 g/mol) single crystal suspension at room temperature. The mixture was allowed to crystallize at room temperature for 28 h. The final suspension was filtered to remove uncrystallized PEO.

Preparation of Patterned AuNP Sheets with Multiple AuNP Frames. First, 0.4 mg of HS−PEO (M_n = 2000 g/mol) was dissolved in 1.0 g of pentyl acetate at 60 °C for 10 min. Then the solution was quenched to 5 °C overnight. The resulted suspension was brought to 38 °C for 10 min to obtain the crystalline seeds. The solution was then left at room temperature to crystallize. Then, 2.0 g of gold colloid in pentyl acetate was added to the PEO solution at t_d = 15 min. The mixture continued to crystallize for 4 days. Subsequently, 1.0 g of 0.04 wt % HS−PEO (M_n = 2000 g/mol) solution in pentyl acetate and 2.0 g of gold colloid in pentyl acetate were added to the mixture. The resultant mixture continued to crystallize for another 5 days. The final suspension was filtered to remove uncrystallized PEO and unbound AuNPs.

Preparation of NP Sheets Consisting of Gold and Magnetite NP. A 1.0 g sample of 0.02 wt % filtered HO−PEO (M_n = 5000 g/mol) single crystal suspension was mixed with 0.2 g of magnetite colloid for 2 h. The mixture was filtered to remove the unbound NPs. 0.5 g of the filtered suspension was mixed with 0.5 g of 0.08 wt % HS−PEO (M_n = 2000 g/mol) solution in pentyl acetate for 24 h before 0.5 g of gold colloid was added. The resultant mixture continued to crystallize at room temperature for another 24 h. The final suspension was filtered to remove uncrystallized PEO and unbound NPs.

Preparation of NP Sheets Consisting of Gold and CdS@ZnS. First, 1.0 g of 0.02 wt % filtered HS−PEO (M_n = 5000 g/mol) single crystal suspension was mixed with 0.3 g of CdS@ZnS colloid for 4 h. The mixture was filtered to remove the unbound NPs. 0.5 g of the filtered suspension was mixed with 0.5 g of 0.08 wt % HS−PEO (M_n = 2000 g/mol) solution in pentyl acetate for 24 h before 0.5 g of gold colloid was added. The resultant mixture continued to crystallize at room temperature for another 24 h. The final suspension was filtered to remove uncrystallized PEO and unbound NPs.

Instrumentation. Transmission electron microscopy (TEM) experiments were conducted on a JEOL 2000FX TEM with an accelerating voltage of 120 kV. UV−vis spectra were collected on an Ocean Optics USB4000 miniature fiber-optic spectrometer.

Results and Discussion. The self-seeding method was used to produce uniform polymer single crystals in a large quantity (Scheme 1a).[37−40] In order to achieve *in situ* NP assembly, tri-*n*-octylphosphine oxide (TOPO) protected AuNPs were added to the HS−PEO/pentyl acetate solution during

Scheme 1. (a) Experimental Procedure of Using the Self-Seeding Method To Grow HS−PEO Single Crystals and (b) Growth Mechanism of AuNP Frames[a]

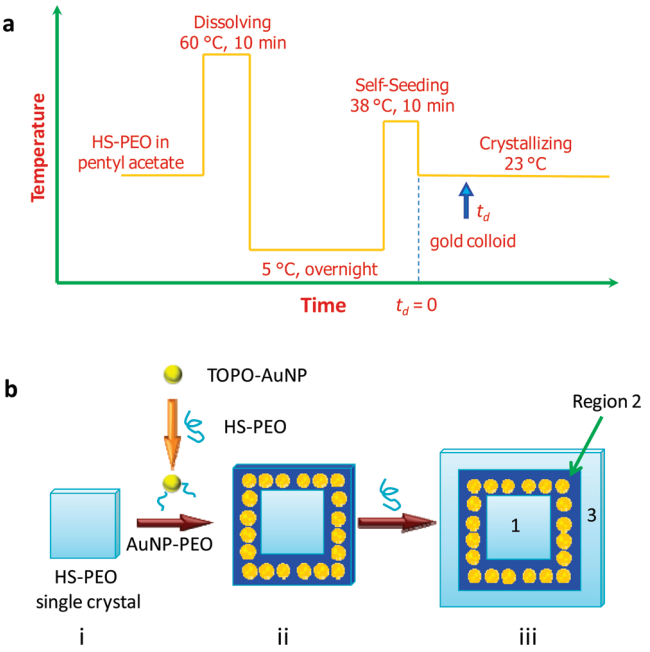

[a] In order to pattern NPs during the growth of the single crystals, AuNP were added at different t_d during HS−PEO crystallization. Key: (i). A HS−PEO lamellar single crystal, which has already formed prior to the addition of gold colloid. The PEO chains are parallel to the lamellar normal and the thiol groups are on the crystal surface. As gold colloid is added to the HS−PEO solution, AuNP−PEO conjugates are formed via the place exchange reaction. The AuNP−PEO conjugates crystallize around the already formed single crystals, generating AuNP frames (ii). After these conjugates are exhausted, PEO continue to crystallize around the AuNP frames, forming a blank margin (iii). 1, 2, and 3 in part iii denote the three distinct regions of the pattern.

the crystallization process. The arrow in the scheme denotes the delay time (t_d) of AuNP addition after the crystallization began. By varying t_d, very different morphologies were observed after approximately 24 h of crystal growth (Figure 1). When AuNPs were added at the beginning of the crystallization, t_d = 0 min, they assembled into a square pattern at the center of the HS−PEO single crystal (denoted by the dash lines), leaving a "blank margin" (free of AuNP) with a width of ~0.8 μm around the crystal edges (Figure 1a). Figure 1b shows the boundary of these two areas. This morphology is different from the previously reported AuNP sheets, where the entire surface of the single crystals was covered by AuNPs, as shown in Figure 1c,d for comparison. When AuNPs were added at t_d = 10 min, AuNP "frames" were formed (Figure 1e). In addition to the margin area around the crystal edges, there is a "blank" area of ~ 0.3 × 0.3 μm at the center of the crystal as well. For t_d = 20 and 30 min, AuNPs assembled into similar frame-like patterns while the central blank squares became larger and larger (~1.2 × 1.2 μm and 2.2 × 2.2 μm, respectively), as shown in Figure 1f,g. Note that there are dark dots at the centers of the single crystals as shown in Figure 1. These dots may be formed by seeds of the single crystals.

Of interest is how AuNPs assembled into these frame patterns. The single crystal with AuNP frame can be divided into three regions as shown in Figure 1g. AuNPs selectively gathered in region 2. Figure 1h shows the enlarged image of the boundary between regions 1 and 2. The lack of AuNP in region 3 suggests complete consumption of AuNP at the late

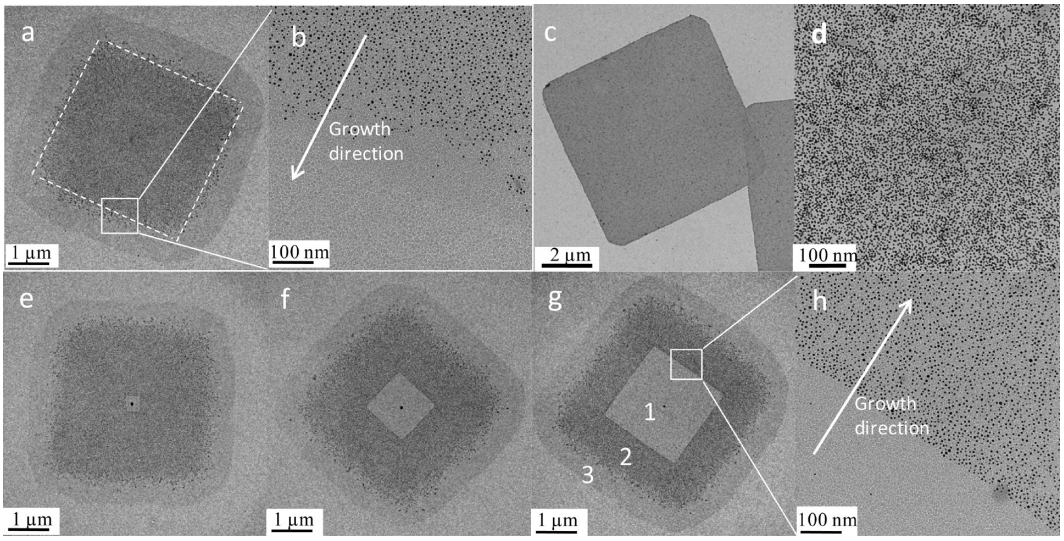

Figure 1. TEM images of AuNP patterns formed on HS−PEO single crystals by varying t_d. Gold colloid was added to HS−PEO solution at t_d = (a) 0 min (e) 10 min, (f) 20 min, and (g) 30 min after HS−PEO began to crystallize. Parts b and h show enlarged images of parts a and g, respectively. Parts c and d show the AuNP sheets with full coverage obtained by mixing the filtered HS−PEO single crystals with AuNPs.

stage of the crystal growth. This was visually confirmed by the color change of the crystallizing solution from wine red to clear. The question then is why AuNPs were immobilized onto region 2, not 1? AuNPs used in our experiment were mainly coated with TOPO, which can be readily replaced by HS−PEO. As these TOPO−AuNPs are added to the crystallizing HS−PEO, they can undergo place exchange reaction with either HS−PEO single crystals or uncrystallized HS−PEO molecules in solution. The increased size of region 1 at longer t_d indicates that regions 1 and 2 were formed *before* and *after* AuNP addition, respectively. The lack of AuNPs in region 1 suggests that most TOPO−AuNPs reacted with uncrystallized HS−PEO molecules, leading to the formation of PEO−AuNP conjugates, as shown in Scheme 1b. Because of the steric hindrance imposed by the attached PEO chains, these PEO−AuNP conjugates could not adsorb onto the already formed single crystals (region 1) under our experimental condition. Nevertheless, these PEO−AuNP conjugates possess improved ability to crystallize, because the increased local concentration of PEO around AuNP facilitated polymer crystallization. Since PEO molecules were tethered to AuNPs, the latter were brought to the single crystal surface as PEO crystallized, forming the AuNP frames. This hypothesis was confirmed by the following observations. At room temperature and within 24 h, HS−PEO (M_n = 2000 g/mol) was unable to homogeneously crystallize from a 0.08 wt % solution. However, once it was mixed with gold colloid, square HS−PEO single crystals were formed readily and these crystals were covered with a dense layer of AuNPs, as shown in Figure 2a. The surface plasmon band of AuNPs shifted from ~520 to ~540 nm as the mixing time increased from 10 min to 7 h, indicating more and more AuNPs were assembled densely on the single crystals (Figure 2b). The proposed growth mechanism for AuNP frames is detailed in Scheme 1b. Two control experiments were conducted to further verify this conjecture. In the first experiment, HS−PEO and TOPO−AuNPs were added subsequently to a suspension of preformed HS−PEO single crystals (Figure 2c). In the second one, presynthesized AuNP−PEO conjugates were added to a suspension of preformed HS−PEO single crystals (Figure 2d). In both cases, the preformed HS−PEO single crystals served as crystalline seeds and similar frame-like patterns were obtained. These results confirmed that AuNP frames were formed by the crystallization of AuNP−PEO conjugates.

Clearly understanding the growth mechanism of AuNP frames paves the way to programming patterns of the aforementioned NP assembly. The NP patterns can be precisely tuned by adjusting four experimental parameters such as the delay time of AuNP addition, crystallization time, AuNP concentration, and the number of AuNP additions, as shown in Figure 3. We took the AuNP frame observed in Figure 1 as a reference pattern. As we advanced the delay time of AuNP addition, region 1 shrank (Figure 3a,b) and smaller blank cores were obtained. As we shortened the crystallization time of the AuNP−PEO conjugates, region 2 shrank and the width of the AuNP frame decreased (Figure 3c,d). As we reduced the AuNP concentration, the AuNP frame was also narrowed and region 3 remained (Figure 3e,f). When the AuNP concentration was reduced, less AuNPs were available to form AuNP frames. As a result, the width of the frames was reduced. After the AuNPs were exhausted, the uncrystallized HS−PEO chains continued crystallizing around the single crystals, forming region 3. As we increased the number of AuNP additions, a new AuNP frame was produced in the outer area (Figure 3g,h). A close look at Figure 3, parts d and f reveals that AuNP chains with the width of one or two NPs were obtained (Figure 4). The AuNP chain in Figure 3f was achieved by reducing the AuNP concentration. The AuNP concentration in the mixed suspension was controlled by the amount of gold colloid added to the crystallizing solution. In experiments to grow the typical AuNP frames, 0.5 g of gold colloid was added to 3.0 g of the crystallizing solution. In order to produce the AuNP chains, 0.1 g of gold colloid was used. These AuNP frames represent a unique type of free-standing, programmable and hierarchical NP assembly. Three features at different length scales can be controlled: the frame size (width and length) and the interframe distance can be varied by controlling crystallization conditions; the inter-NP distance could be controlled by varying the polymer chain length.[32]

In situ patterning NPs during polymer crystallization also allowed us to assemble multiple types of NPs on one single crystal. From Scheme 1b, if PEO with different end functional groups can cocrystallize, multiple types of NPs can

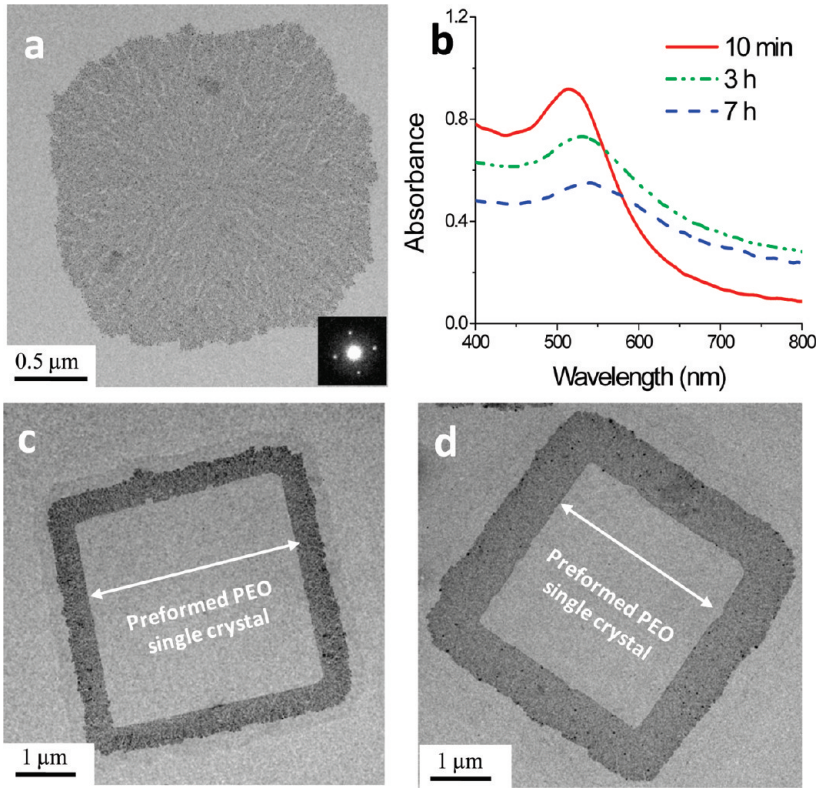

Figure 2. Crystallization of AuNP−PEO hybrids. (a) Single crystal formed by AuNP−PEO hybrids. Inset shows the selected area electron diffraction. (b) UV−vis spectra of the mixture of AuNP and HS−PEO at various mixing times. (c and d) AuNP frame formed by using preformed HS−PEO single crystals as the seeds. The mixture of AuNP and HS−PEO was used in part c, while PEO−AuNP hybrids were used in part d.

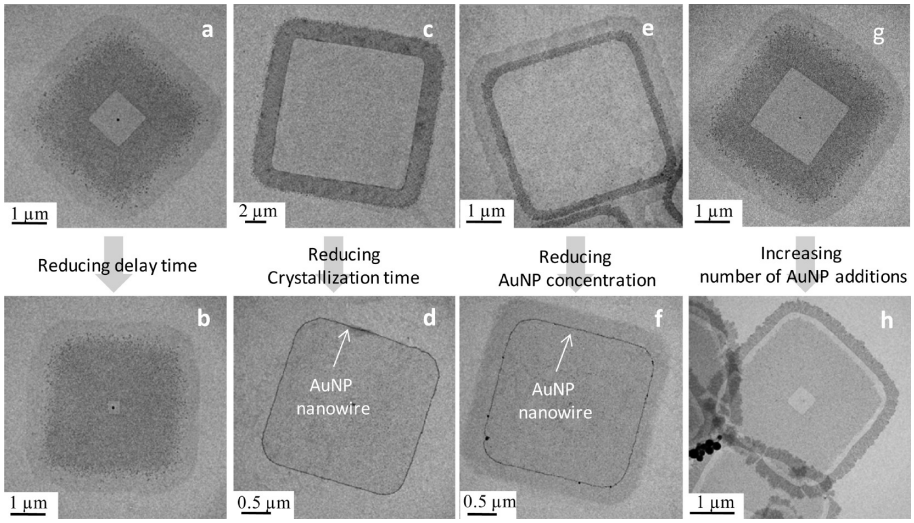

Figure 3. TEM images of a series of patterns formed on AuNP sheets by varying experimental parameters, including the delay time of AuNP addition (a, b), crystallization time (c, d), AuNP concentration (e, f) and number of AuNP additions (g, h).

then be assembled in one single crystal with desired patterns. As a proof-of-concept, HO−PEO single crystals (M_n = 5000 g/mol) were mixed with iron(II, III) oxide (magnetite) NPs to form the NP cores, which were used as crystalline seeds to further grow AuNP frames by subsequently adding HS−PEO solution and gold colloid into the system. Figure 5a shows the obtained binary NP sheet. The inner dark square (~3 × 3 μm) consists of magnetite NPs, which are about 15 nm in diameter (Figure 5b). The outer dark frame (~0.3 μm in width) is made of AuNP, shown in Figure 5c. The width of the middle gray stripe (inter-domain distance) was determined by the interval between the additions of HS−PEO and gold colloid. By following the similar assembling procedure, semiconducting quantum dots (CdSe@ZnS) were assembled with AuNP as well (Figure 5d,e).

Figure 5f shows the schematics of the binary NP sheet. Both examples clearly demonstrated our ability to spatially pattern various NPs to different domains on one single crystal. These novel hybrid structures are multifunctional with properties of both NPs. For magnetite NPs/AuNPs/polymer single crystals, the hybrids can be actuated using an external magnetic field while they can also be used for sensing or catalytic purposes because of AuNPs. For CdSe@

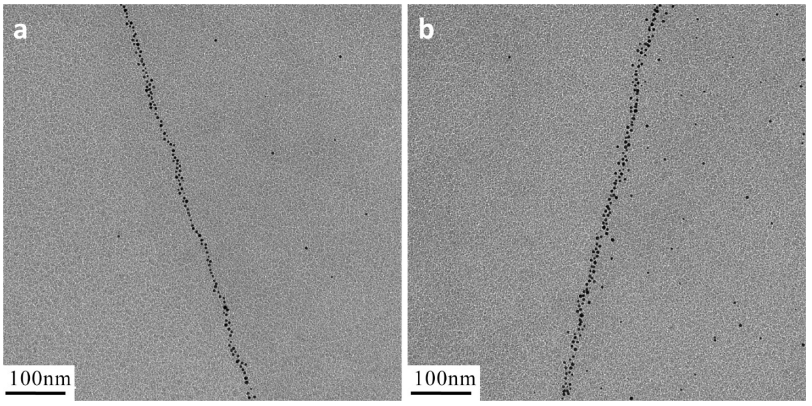

Figure 4. TEM images of the enlarged area for Figure 3d (a) and Figure 3f (b) showing the AuNP chain formation.

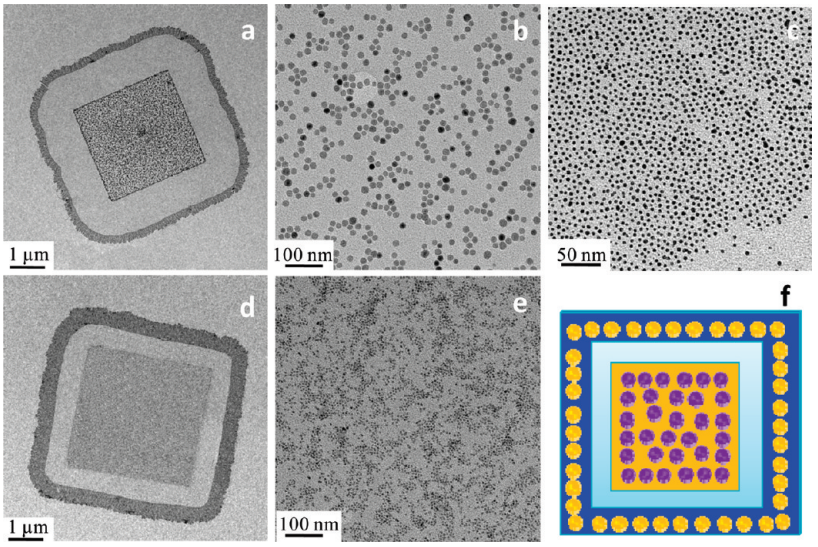

Figure 5. TEM images of the binary NP sheets consisting of two types of NPs. (a) AuNP/magnetite NP binary sheets. The inner square is covered by magnetite NPs (b) and the outer frame is made of AuNPs (c). (d) AuNP/CdSe@ZnS binary sheets. The inner square is covered by CdSe@ZnS (e) and the outer frame is made of AuNPs similar to part c. (f) Schematic representation of the binary sheets. Three features of the pattern at different length scales in part f can be controlled, namely, the inter-NP distance, the width, and the length of each NP domain and the interdomain distance.

ZnS/AuNP/polymer single crystals, CdSe@ZnS can serve as the label to locate the hybrids, which can be used for sensing or catalytic applications.

In conclusion, crystallization of end-functionalized PEO was exploited to produce NP sheets with programmable patterns in a large quantity. AuNP−PEO conjugates were able to crystallize around PEO single crystals to assemble into frames and chains. Binary NP sheets containing magnetite NPs/semiconducting quantum dots and AuNPs were also successful obtained. The ability to pattern various NPs into well-defined domains on a 2D free-standing lamella is unprecedented and it paves the way to multifunctional NP assembly. It is anticipated that these unique NP assemblies can find applications in nanodevices and multifunctional drug delivery systems.

Acknowledgment. This work was supported by the NSF CBET-0730738.

References and Notes

(1) Alivisatos, A. P. *Science* **1996**, *271*, 933–937.
(2) Murray, C. B.; Kagan, C. R.; Bawendi, M. G. *Annu. Rev. Mater. Sci.* **2000**, *30*, 545–610.
(3) Daniel, M. C.; Astruc, D. *Chem. Rev.* **2004**, *104*, 293–346.
(4) Bockstaller, M. R.; Mickiewicz, R. A.; Thomas, E. L. *Adv. Mater.* **2005**, *17*, 1331–1349.
(5) Balazs, A. C.; Emrick, T.; Russell, T. P. *Science* **2006**, *314*, 1107–1110.
(6) Srivastava, S.; Kotov, N. A. *Soft Matter* **2009**, *5*, 1146–1156.
(7) Claridge, S. A.; Castleman, A. W.; Khanna, S. N.; Murray, C. B.; Sen, A.; Weiss, P. S. *ACS Nano* **2009**, *3*, 244–255.
(8) Ofir, Y.; Samanta, B.; Rotello, V. M. *Chem. Soc. Rev.* **2008**, *37*, 1814–1823.
(9) Iakovenko, S. A.; Trifonov, A. S.; Giersig, M.; Mamedov, A.; Nagesha, D. K.; Hanin, V. V.; Soldatov, E. C.; Kotov, N. A. *Adv. Mater.* **1999**, *11*, 388–392.
(10) Wang, Y.; Angelatos, A. S.; Caruso, F. *Chem. Mater.* **2008**, *20*, 848–858.
(11) Nie, Z. H.; Fava, D.; Kumacheva, E.; Zou, S.; Walker, G. C.; Rubinstein, M. *Nat. Mater.* **2007**, *6*, 609–614.
(12) Kang, Y. J.; Erickson, K. J.; Taton, T. A. *J. Am. Chem. Soc.* **2005**, *127*, 13800–13801.
(13) DeVries, G. A.; Brunnbauer, M.; Hu, Y.; Jackson, A. M.; Long, B.; Neltner, B. T.; Uzun, O.; Wunsch, B. H.; Stellacci, F. *Science* **2007**, *315*, 358–361.
(14) Alivisatos, A. P.; Johnsson, K. P.; Peng, X. G.; Wilson, T. E.; Loweth, C. J.; Bruchez, M. P.; Schultz, P. G. *Nature* **1996**, *382*, 609–611.
(15) Mirkin, C. A.; Letsinger, R. L.; Mucic, R. C.; Storhoff, J. J. *Nature* **1996**, *382*, 607–609.
(16) Nykypanchuk, D.; Maye, M. M.; van der Lelie, D.; Gang, O. *Nature* **2008**, *451*, 549–552.

(17) Cheng, W. L.; Campolongo, M. J.; Cha, J. J.; Tan, S. J.; Umbach, C. C.; Muller, D. A.; Luo, D. *Nat. Mater.* **2009**, *8*, 519–525.
(18) Lamm, M. S.; Sharma, N.; Rajagopal, K.; Beyer, F. L.; Schneider, J. P.; Pochan, D. J. *Adv. Mater.* **2008**, *20*, 447–451.
(19) Chai, J.; Buriak, J. M. *ACS Nano* **2008**, *2*, 489–501.
(20) Cui, H. G.; Chen, Z. Y.; Zhong, S.; Wooley, K. L.; Pochan, D. J. *Science* **2007**, *317*, 647–650.
(21) Chiu, J. J.; Kim, B. J.; Kramer, E. J.; Pine, D. J. *J. Am. Chem. Soc.* **2005**, *127*, 5036–5037.
(22) Li, B.; Li, L.; Wang, B.; Li, C. Y. *Nat. Nanotechnol.* **2009**, *4*, 358–362.
(23) Geil, P. H., *Polymer single crystal;* Robert E. Krieger Publishing Co.: Huntington, NY, 1973.
(24) Li, C. Y.; Li, L.; Cai, W.; Kodjie, S. L.; Tenneti, K. K. *Adv. Mater.* **2005**, *17*, 1198–1202.
(25) Li, L. Y.; Li, C. Y.; Ni, C. Y. *J. Am. Chem. Soc.* **2006**, *128*, 1692–1699.
(26) Li, L.; Li, B.; Hood, M. A.; Li, C. Y. *Polymer* **2009**, *50*, 953–965.
(27) Wang, B. B.; Li, B.; Xiong, J.; Li, C. Y. *Macromolecules* **2008**, *41*, 9516–9521.
(28) Li, L. Y.; Yang, Y.; Yang, G. L.; Chen, X. M.; Hsiao, B. S.; Chu, B.; Spanier, J. E.; Li, C. Y. *Nano Lett.* **2006**, *6*, 1007–1012.
(29) Kodjie, S. L.; Li, L. Y.; Li, B.; Cai, W. W.; Li, C. Y.; Keating, M. *J. Macrom. Sci. Phys.* **2006**, *45*, 231–245.
(30) Bassett, G. A. *Phil. Mag.* **1958**, *3*, 1042–1045.
(31) Bassett, G. A.; Blundell, D. J.; Keller, A. *J. Macro. Sci. Phys.* **1967**, *1*, 161–184.
(32) Li, B.; Li, C. Y. *J. Am. Chem. Soc.* **2007**, *129*, 12–13.
(33) Wang, B. B.; Li, B.; Zhao, B.; Li, C. Y. *J. Am. Chem. Soc.* **2008**, *130*, 11594–11595.
(34) Li, B.; Ni, C.; Li, C. Y. *Macromolecules* **2008**, *41*, 149–155.
(35) Green, M.; O'Brien, P. *Chem. Commun.* **2000**, 183–184.
(36) Park, J.; An, K. J.; Hwang, Y. S.; Park, J. G.; Noh, H. J.; Kim, J. Y.; Park, J. H.; Hwang, N. M.; Hyeon, T. *Nat. Mater.* **2004**, *3*, 891–895.
(37) Blundell, D. J.; Keller, A.; Kovacs, A. J. *J. Polym. Sci., Part B* **1966**, *4*, 481–486.
(38) Chen, W. Y.; Li, C. Y.; Zheng, J. X.; Huang, P.; Zhu, L.; Ge, Q.; Quirk, R. P.; Lotz, B.; Deng, L. F.; Wu, C.; Thomas, E. L.; Cheng, S. Z. D. *Macromolecules* **2004**, *37*, 5292–5299.
(39) Chen, W. Y.; Zheng, J. X.; Cheng, S. Z. D.; Li, C. Y.; Huang, P.; Zhu, L.; Xiong, H. M.; Ge, Q.; Guo, Y.; Quirk, R. P.; Lotz, B.; Deng, L. F.; Wu, C.; Thomas, E. L. *Phys. Rev. Lett.* **2004**, *93* (028301), 1–4.
(40) Cai, W.; Li, C. Y.; Li, L.; Lotz, B.; Keating, M.; Marks, D. *Adv. Mater.* **2004**, *16*, 600–605.